Investigating the Accuracies in Short-Term Weather Forecasts and Its Impact on Irrigation Practices

Shubham Gedam[1]; Harshavardhan Pallam[2]; B. V. N. P. Kambhammettu[3]; Varaprasad Anupoju[4]; and Satish K. Regonda[5]

Abstract: The effectiveness of irrigation schedules and crop growth models is largely dependent on the accuracies associated with the most uncertain input parameter, viz. weather forecasts. This research is focused on quantifying the inaccuracies associated with the India Meteorological Department (IMD) issuing short-term weather forecasts (with 1–5 days lead time), and their propagation into irrigation models, with an objective to select the optimal parameters for use with simulation. While precipitation (P) forecasts were directly used, remaining meteorological forecasts were converted to reference evapotranspiration (ET_0) forecasts. The effectiveness of the 'P' and 'ET_0' forecasts was found to be low at all lead times. We applied two popular bias correction methods: linear scaling (LS) and empirical quantile mapping (EQM), and observed a marginal improvement in forecast skill. Bias-corrected, forecast-driven irrigation scenarios, along with conventional irrigation (that ignores weather forecast), and a hypothetical perfect 5-day forecast-based irrigation (as reference) system were tested on a water-intensive paddy crop for two growing seasons (S1: monsoon and S2: winter). Conventional irrigation resulted in the highest use of irrigation water (820 mm in S1, 880 mm in S2) and percolation loss (1,140 mm in S1, 680 mm in S2), while achieving a low relative yield (0.88 in S1, 0.87 in S2). LS-corrected forecasts outperformed other scenarios with 20.24% ± 4.21% and 1.25% ± 1.51% savings in irrigation costs for S1 and S2, respectively. While IMD forecasts greatly improved irrigation schedules in the monsoon season, their usage for winter crops was found to be trivial. Our findings conclude that LS-corrected IMD forecasts were moderately reliable over multiple lead times and can serve as a valuable addition to irrigation scheduling, provided the contribution of 'P' to the total water balance is significant. **DOI: 10.1061/JWRMD5.WRENG-5644.**

Author keywords: India Meteorological Department (IMD); Weather forecast; Bias correction; Irrigation schedule; Crop simulation; Rice.

Introduction

India's water withdrawal for agriculture (~700 billion cubic meters (BCM)/year) is the highest in the world, far higher than the combined utilization of the next two ranked countries, i.e., China and US (FAO 2017). Two crops, namely rice (paddy) and sugarcane, occupy one-fourth of India's gross cropped area and consume over 60% of total irrigation supplies (Sharma et al. 2018). Globally, India ranks first in area under rice cultivation (~45 million hectares 'M ha') as well as rice water consumption (~221 BCM), and second in rice production (~160 M tons). Despite these encouraging statistics, crop productivity (CP: yield per unit area), and crop water productivity (CWP: yield per unit of water delivered) of rice in India (3.6 t ha^{-1} and 0.495 kg m^{-3}) are substantially lower than corresponding world averages (4.6 t ha^{-1} and 0.755 kg m^{-3}) (Chapagain and Hoekstra 2011). A number of studies have shown that India experiences high production loss, a shortfall of freshwater resources, and a reduction in the share of agricultural water due to population growth, changes in climate, and increased urbanization (Auffhammer et al. 2006; Cline 2007; Aggarwal 2008; Mishra et al. 2013). These situations clearly highlight the need to improve CWP in agriculture by saving irrigation water and maintaining crop production (Boutraa 2010). Sustainable irrigation strategies help to improve CWP by analyzing soil-water-crop-weather interactions on a real-time basis (Nikolaou et al. 2020). In India, irrigation scheduling is mostly driven by farmers' intuitive decisions based on the availability of resources and established practices. Such scheduling activities largely ignore the weather conditions between irrigations, hence failing to optimize water use in agriculture. Accounting for weather forecasts can modify the decision on irrigation timing and amount, which consequently result in optimal utilization of irrigation water to achieve higher production (Wang and Cai 2009; Cai et al. 2011; Hejazi et al. 2014).

India Meteorological Department (IMD)-issued short-term weather forecasts (with 1 to 5 days lead time) provide an opportunity to analyze crop water requirements in response to future weather, thereby helping to optimize irrigation strategies. IMD issues daily operational weather forecasts at the block-level using a high-resolution, deterministic, global forecast system model (GFS T1534). The model runs daily for 10 days into the future and provides outputs at three-hour intervals. The forecast datasets

[1]M.Tech Scholar, Dept. of Civil Engineering, Indian Institute of Technology Hyderabad, Kandi, Sangareddy, Telangana 502284, India (corresponding author). Email: ce20mtech11016@iith.ac.in; shubhamgedam55@gmail.com

[2]M.Tech Scholar, Dept. of Civil Engineering, Indian Institute of Technology Hyderabad, Kandi, Sangareddy, Telangana 502284, India. Email: ce20mtech11011@iith.ac.in

[3]Associate Professor, Dept. of Civil Engineering, Indian Institute of Technology Hyderabad, Kandi, Sangareddy, Telangana 502284, India. Email: phanindra@ce.iith.ac.in

[4]Assistant Professor, Dept. of Civil Engineering, Maharaj Vijayaram Gajapathi Raj College of Engineering, Vizianagaram, Andhra Pradesh 535005, India. ORCID: https://orcid.org/0000-0001-8234-8438. Email: varaprasad.a@gmail.com; ce13p0001@iith.ac.in

[5]Assistant Professor, Dept. of Climate Change and Dept. of Civil Engineering, Indian Institute of Technology Hyderabad, Kandi, Sangareddy, Telangana 502284, India. Email: satishr@ce.iith.ac.in

Note. This manuscript was submitted on November 22, 2021; approved on September 14, 2022; published online on November 23, 2022. Discussion period open until April 23, 2023; separate discussions must be submitted for individual papers. This paper is part of the ***Journal of Water Resources Planning and Management***, © ASCE, ISSN 0733-9496.

are published each day at 08:30 a.m. for the next 5 days. Evaluation of the GFS T1534 model revealed that the model broadly captures heavy rainfall events during monsoon, but significantly overestimates low rainfall events both in number and in magnitude (Mukhopadhyay et al. 2019). Reasonable forecasting skill was observed for all rainfall categories, but the skill was found to decrease with lead time (Mukhopadhyay et al. 2019). Evaluation of forecasts of other meteorological variables has not been found in the literature, which may be due to the fact that a large number of applications such as climate change impact studies (Chen et al. 2013a, b), hydrologic analysis of stream flows (Tiwari et al. 2022), and extreme event analysis (Maity et al. 2019) use exclusive precipitation forecasts with reasonable accuracy. However, irrigation schedules and crop growth models demand evapotranspiration (*ET*) forecasts in addition to precipitation (*P*) forecasts for the effective management of water in agriculture (Wang and Cai 2009). This is particularly true with the cultivation of water-intensive crops like rice and sugarcane, where the contribution of *ET* to total agricultural water is significant (Sharma et al. 2018). Being the key hydrologic contributor to the water balance, an accurate prediction of reference *ET* (ET_0) using a standard method, such as FAO Penman–Monteith, from the available meteorological forecasts is essential to effectively manage crop water (Cai et al. 2007). However, the nonavailability of solar radiation data by most of the public weather forecast agencies, including IMD, has promoted the development of soft computing models (Kumar et al. 2002; Landeras et al. 2009) and temperature-driven empirical models (Luo et al. 2014; Xiong et al. 2016; Ballesteros et al. 2016) for ET_0 forecasts. All of these models were proven to be less effective in estimating ET_0 as the meteorological drivers for ET_0 such as wind speed, humidity, and solar radiation data were not considered (Yang et al. 2016). The analytical method (AM) proposed by Cai et al. (2007) overcomes this limitation by translating available cloud cover (CC) into solar radiation, thus making full use of available meteorological forecasts. A number of studies have concluded that the use of public weather forecasts in the Penman–Monteith equation through AM can significantly improve the performance of daily ET_0 forecasts (Yang et al. 2016, 2019; Anupoju et al. 2021).

Evidence of bias in '*P*' and 'ET_0' forecasts has prompted many researchers to avoid the direct use of publicly available weather forecasts in crop simulation models (Venäläinen et al. 2005; Ines and Hansen 2006). Thus, post-processing of weather forecasts, such as bias correction, became a pre-requisite for their use in irrigation management studies (Tiwari et al. 2022). Bias correction techniques are designed to either reduce or remove the errors (that are of systematic in nature) associated with the forecasts, thereby increasing the skill and reliability of weather forecasts. Bias correction techniques are broadly categorized into two groups, i.e., (1) linear methods, which adjust the means of raw forecasts to match with observations using the difference or ratio of the two means applied as a correction factor, and (2) distribution methods, which adjusts raw forecasts by mapping the statistical distribution of observed values onto forecasted values for each quantile (Crochemore et al. 2016). Bias correction techniques have been widely used for various applications, and reviews of different bias correction techniques in hydrology and agriculture can be found in the literature (Lafon et al. 2013; Pierce et al. 2015; Dang et al. 2017). Typically, an appropriate bias correction technique is selected by evaluating the propagation of error associated with a given forecast scenario into the model outputs (Lafon et al. 2013; Chen et al. 2021).

A number of studies have evaluated the role of '*P*' forecasts in irrigation schedules and crop yields using deterministic (Wang and Cai 2009; Mishra et al. 2013) and stochastic (Cai et al. 2011; Jamal et al. 2018, 2019) optimization techniques. The utility of ET_0 forecasts for real-time irrigation management is demonstrated by a number of researchers including Snyder et al. (2009), Luo et al. (2014), Traore et al. (2016), and Yang et al. (2016, 2019), but only a few studies have focused on the combined use of '*P*' and 'ET_0' forecasts in irrigation schedules and crop simulation models (Anupoju et al. 2021; Chen et al. 2021). However, none of these studies have either quantified or adjusted the bias in raw forecasts prior to their use in irrigation schedules. This motivates the present study, and the objectives of this study are as follows: (1) assess the reliability of IMD-issued precipitation forecasts and estimated ET_0 forecasts at different lead times, (2) evaluate the performance of two bias correction techniques in reducing systematic errors and consequently improving forecast skill, (3) analyze water balance and crop yield fluxes under conventional and forecast-assisted rule-based irrigation scenarios, and (4) select an optimal forecast horizon and bias correction technique in using IMD forecasts for irrigation scheduling. The results of this paper are expected to provide guidelines for real-time management of irrigation water using IMD short-term weather forecast datasets. The conceptual framework of the proposed research is illustrated in Fig. 1.

Methodology

Study Area

Meteorological, phenological, and management conditions were observed for one agricultural year (June 1, 2019–May 31, 2020) in a private farmland situated in the Nandi Kandi village of the Sangareddy district, Telangana, India (17°36′50″ N, 77°59′15″ E, 525 m above sea level). As per Kö ppen-Geiger classification, the region falls under tropical savanna climate zone (Aw) characterized by lengthy dry and short wet seasons (Kottek et al. 2006). The mean annual precipitation of the region is 900 mm, and most of the annual precipitation (~75%) occurs during the south-west monsoon (July–September). Maximum temperatures (32 to 45°C) are observed during summer (March–June), whereas minimum temperatures (15 to 24°C) are seen in winter (December–February). The humidity of the region varies from 35% in summer to 73% during monsoon season (CGWB 2013). Soils of the site have a sandy loam texture with a mean bulk density of 1.58 g cm^{-3}, saturated water content of 0.44 cm^3 cm^{-3}, field capacity of 0.31 cm^3 cm^{-3}, permanent wilting point of 0.12 cm^3 cm^{-3}, and mean saturated hydraulic conductivity of 0.192 m day^{-1} (Anupoju and Kambhammettu 2020).

Rice is the second largest cultivated crop in the region after cotton and is grown in two seasons: rain-fed 'Kharif' (monsoon): S1, and irrigated 'Rabi' (winter): S2. Kharif cultivation of rice is more prominent due to frequent rain spells and favorable agro-climatic conditions. The 'BPT-5204' variant of rice was transplanted from a nursery and planted in the field with a spacing of 15 to 20 cm. The phenology, growth stages, and water requirement of the crop are provided in Table 1. Irrigation scheduling is done at 4–6 day intervals, with timing and amount decided based on the farmer's intuitive knowledge. Conventional irrigation (CI) practiced in the region does not utilize weather forecast information between the irrigations and is driven solely by resource availability. Farmers used to apply a fixed amount of irrigation at regular intervals resulting in huge wastes of water and electricity.

Data Collection and Processing

India Meteorological Department (IMD) is the nodal agency that monitors and archives various meteorological variables, and issues

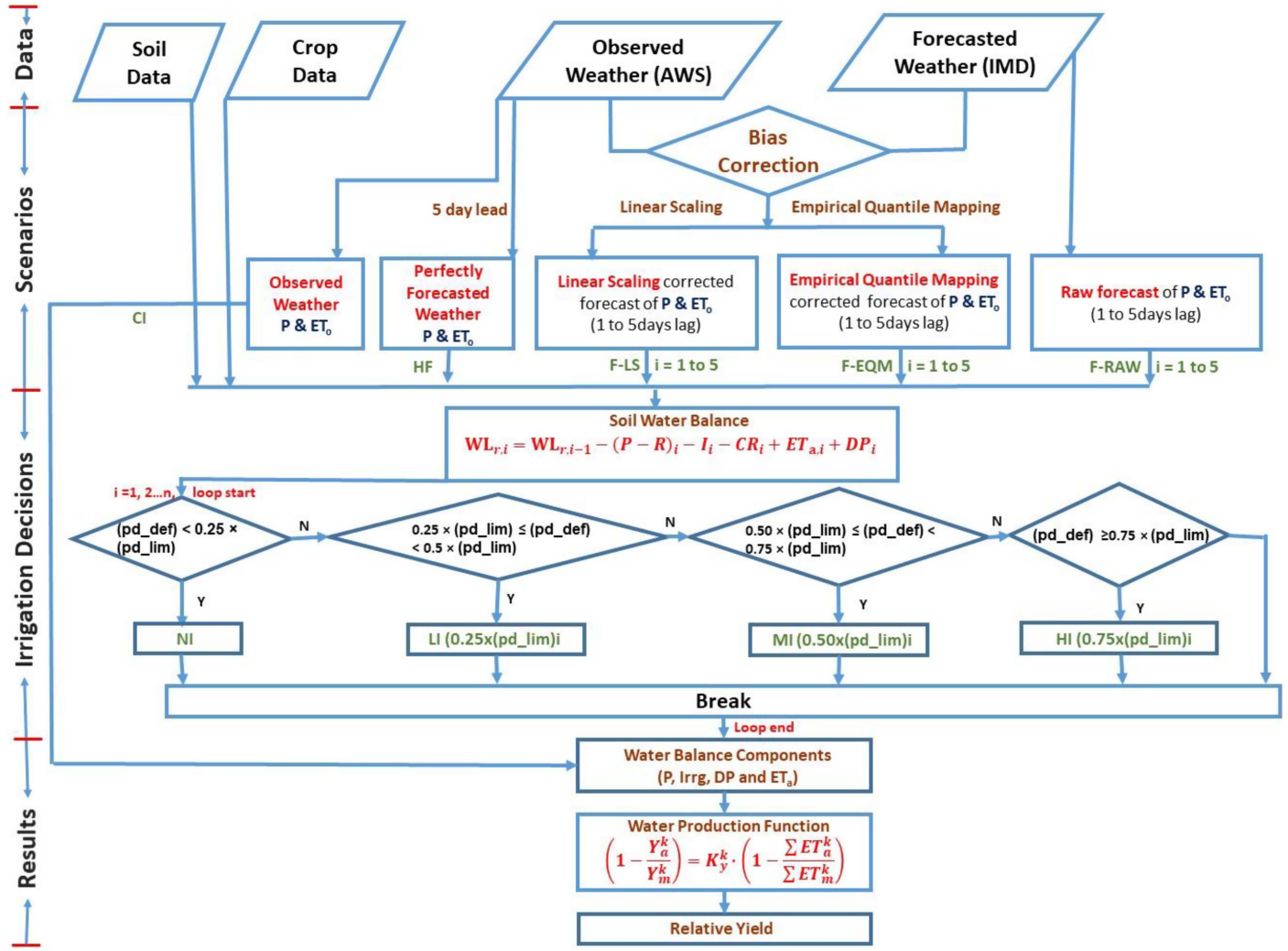

Fig. 1. Flowchart illustrating the methodology to evaluate the role of bias-corrected IMD weather forecasts in irrigation schedules and crop growth simulations.

Table 1. Stage-specific crop coefficients and yield response factors of rice considered in the water balance model

Growth stage	Period (days)	Limiting ponding depth (mm)	Water requirement (mm)	Crop coefficient (Kc)	Yield response factor (Ky)
Transplantation	20	50	250	1.10	0.80
Vegetative	40	30	450	1.13	1.03
Reproduction	30	50	400	1.04	0.80
Ripening	20	10	100	0.73	0.45

weather forecasts. IMD's short-term weather forecasts are based on a suite of operational numerical weather prediction (NWP) models and made available to the public at the block (mandal) level for the next 1–5 days (https://mausam.imd.gov.in/). The IMD's published weather forecasts consist of the following meteorological variables: precipitation (P), maximum temperature (T_{max}), minimum temperature (T_{min}), maximum humidity (RH_{max}), minimum humidity (RH_{min}), wind speed (w), wind direction, and cloud cover (CC). Data for one agricultural year (i.e., June 1, 2019–May 31, 2020) was considered in this study. An automatic weather station (AWS) (Spectrum Technologies, US, Model: 2900ET) located about 12 km east of the experimental plot was used to monitor meteorological variables on a daily basis. An open-path eddy covariance (EC) flux tower was installed in the experimental plot to monitor high-frequency water vapor (H_2O) flux using a fast response infrared gas analyzer (IRGASON-EB-IC, Campbell Sci. Inc., US) and a 3D sonic anemometer. The flux data is sampled at a 10-Hz frequency, averaged over 30 min, and presented as daily means of evapotranspiration (ET_a) for use with calibration.

ET_0 Estimation from Weather Forecasts

The unavailability of solar radiation forecasts limits the use of the universally accepted FAO Penman–Monteith (FAO-PM) method in estimating reference evapotranspiration (ET_0) forecasts. To overcome this limitation, the analytical method proposed by Cai et al. (2007) was adopted by translating the available IMD forecasts of CC into solar radiation. This will ensure a fair utilization of a full range of IMD meteorological forecasts in representing the key hydrological fluxes of the water balance equation, viz, P and ET_0. The FAO-PM equation for the estimation of daily ET_0 (mm day^{-1}) considering a hypothetical reference crop (Allen et al. 1998, 2006) is as follows:

$$ET_0 = \frac{0.408\Delta(R_n - G) + \gamma\frac{900}{T+273}u_2(e_s - e_a)}{\Delta + \gamma(1 + 0.34u_2)} \quad (1)$$

where T is mean air temperature (°C), u_2 is wind speed at a height of 2 m from the surface (m s^{-1}), e_a and e_s are, respectively, the actual and saturated vapor pressures of air above the surface (kPa), G is soil heat flux density (MJ m^{-2} day^{-1}) that can be ignored for daily simulations, R_n is net radiation at crop surface (MJ m^{-2} day^{-1}), Δ is the slope of the vapor pressure curve (kPa °C^{-1}), and γ is the psychometric constant (kPa °C^{-1}). Except R_n, all other variables can be directly obtained from IMD-published datasets. Net radiation is computed as the difference between net shortwave and net longwave radiation and given by

$$R_n = R_{ns} - R_{nl} \quad (2)$$

where R_{ns} is considered as a fraction of solar radiation (R_s) given by

$$R_{ns} = (1 - \alpha)R_s \quad (3)$$

where α is the albedo of reference crop (0.23). Shortwave radiation (R_s) is obtained from sunshine duration (n) using the Angstrom equation and given by

$$R_s = \left(a + b_s \cdot \frac{n}{N}\right)R_a \quad (4)$$

where R_a is extraterrestrial radiation, n is actual duration of sunshine, and N is daylight duration, and a and b_s are non-dimensional parameters representing the part of R_a reaching earth. The AM method considers a linear inverse relationship between 'n' and 'CC' with $n = N$ on a clear day to $n = 0$ on an overcast day. Region-specific crop coefficients (K_c) for rice were used to convert ET_0 forecasts into crop ET (ET_c) forecasts for use with soil-water balance studies (Anupoju and Kambhammettu 2020).

Bias Correction Methods

It is a known fact that forecasts are associated with an error (bias) that can be reduced by applying appropriate bias correction techniques. In this paper, two bias correction methods were applied, i.e., linear scaling (LS) and empirical quantile mapping (EQM). The first method, LS, adjusts raw forecasts using a multiplicative factor, equal to the ratio of the observed to forecast means and given by

$$P_{cor} = P_{raw} \cdot \frac{\overline{P_{obs}}}{\overline{P_{raw}}} \quad (5)$$

$$ET_{cor} = ET_{raw} \cdot \frac{\overline{ET_{obs}}}{\overline{ET_{raw}}} \quad (6)$$

where the subscripts 'obs', 'raw', and 'cor' correspond to observed values, raw forecasts, and corrected forecasts, respectively. The second method, EQM, adjusts forecasts by mapping statistical distributions of forecasts and observations. At first, the cumulative distribution function (CDF) of observations is divided into a number of discrete quantiles. Raw forecasts are then resampled to match with the frequency of the observed CDF with the same quantile value. We used quantiles of 10 percentiles for the observed and forecasted datasets and applied bias correction for each bin. The presence of a significant number of zeros in precipitation, particularly for regions dominated by monsoons, poses challenges, similar to those in this study. For example, whether to treat zero and non-zero precipitation values separately or jointly is subjective (Maity et al. 2019). In this study, all precipitation data that consists of both zero and non-zero precipitation values are considered so that the bias-corrected forecasts can be smoothly integrated with irrigation models. Among the two methods, the LS method is relatively simple and improves the first moment of forecasts (mean), but significantly distorts other moments of distribution (Arnell 2003; Lafon et al. 2013). The EQM method modifies forecasts such that the adjusted forecast will have similar distribution aspects as the observed values; however, it may lead to higher bias after correction if a mismatch in the data pairs exists, yet preserving the shape (Lafon et al. 2013).

Evaluation of Forecasts

All three forecasts, i.e., raw, LS-corrected and EQM-corrected forecasts for both P and ET_0 were evaluated at all lead times using three metrics, i.e., multiplicative bias (BIAS), root mean squared error (RMSE), and correlation coefficient (ρ). Each of these metrics evaluate a different aspect of the forecast. Bias is a measure of the factor by which climatological forecasts ($\bar{F}$) deviate from climatological observations ($\bar{O}$), and is given by

$$\text{BIAS} = \frac{\bar{F}}{\bar{O}}, \text{where } \bar{F} = \frac{\sum_{i=1}^{n} F_i}{n} \quad \text{and} \quad \bar{O} = \frac{\sum_{i=1}^{n} O_i}{n} \quad (7)$$

The difference between forecast and corresponding observation is termed as 'error,' and it provides information on forecast accuracy. While multiple error metrics such as mean error, mean absolute error, and RMSE were available, RMSE was used in this study. The RMSE allows one to comment on the forecast accuracy by penalizing large errors relatively heavily and is calculated as follows:

$$\text{RMSE} = \sqrt{\frac{1}{n}\sum_{i=1}^{n}[F_i - O_i]^2} \quad (8)$$

where F_i and O_i are the forecast and corresponding observed value, respectively, and 'n' is the number of data points. The Pearson correlation coefficient (ρ) quantifies the linear association between forecasts and corresponding observations and is given by

$$\rho = \frac{\frac{1}{N}\sum_{i=1}^{n}(F_i - \bar{F}) \cdot (O_i - \bar{O})}{S_F \cdot S_O} \quad (9)$$

where S_F and S_O correspond to the standard deviations of forecasts and observations, respectively. An accurate forecast should yield a bias of one, RMSE of zero, and ρ of one.

Crop Water and Yield Dynamics

A total of five scenarios with observed, raw forecasts, and bias-corrected forecast sets of 'P' and 'ET_0' were considered to analyze water balance and yield dynamics during crop growth. These scenarios can be described as:

1. Conventional irrigation (CI)—irrigation practiced in the region based on the farmers' knowledge and established practices. This method does not use any kind of weather forecasts or irrigation decisions;
2. Hypothetical perfect forecast-based irrigation (HF)—crop simulation model run in the past in retrospective mode using observed values as future forecasts, and is considered as the reference scenario;
3. Raw forecast-based irrigation (F-RAW)—crop simulation model with rule-based irrigation schedules considering raw weather forecasts at different lead times;
4. LS-corrected, forecast-based irrigation (F-LS)—crop simulation model with rule-based irrigation schedules considering LS-corrected P and ET_0 forecasts at different lead times; and

5. EQM-corrected, forecast-based irrigation (F-EQM)—crop simulation model with rule-based irrigation schedules considering EQM-corrected P and ET_0 forecasts at different lead times.

A simple water balance model conserving various fluxes of water entering and leaving the field plot was applied for each time step during the crop period as

$$(WL_i - WL_{i-1}) = (P_i + \mathrm{Irr}_i) - (ET_i - DP_i) \quad (10)$$

where WL_i and WL_{i-1} are the field water depths (mm) at the end of day 'i' and 'i-1', with the difference term $(WL_i - WL_{i-1})$ representing ponding deficit, i.e., the depth by which the field is short of required ponding (Table 2). P_i, Irr_i, ET_i, and DP_i correspond to precipitation, applied irrigation, actual evapotranspiration, and deep percolation at the end of day 'i', and are all represented in 'mm' of water. Actual ET was calculated from the crop coefficient (K_c) approach, with stage-specific (K_c) values taken from Anupoju and Kambhammettu (2020) (Table 1). The rice fields are grown under submerged conditions, so the effect of water stress coefficient (K_s) is not considered. Deep percolation for each day is computed from Darcy's law with a hydraulic gradient derived from the available ponding depth. One of the possible four irrigation depths (NI: no irrigation, LI: light irrigation, MI: medium irrigation, HI: high irrigation) is triggered for each time step using a set of '*if-then*' rules with an objective to bring the ponding depth back to the limiting value (Table 2). CI is accompanied with a fixed irrigation amount and frequency and is guided by the availability of resources. Similarly, forecast scenarios estimate irrigation amount to compensate ponding deficit. Hence, differences in water fluxes between CI and forecast-based scenarios are attributed to the combined effect of weather forecast and irrigation decisions. To highlight the benefits of CI alone, an additional scenario with rule-based irrigation decisions in the absence of weather forecast was considered.

Table 2. Rule-based irrigation schedules considered in the water balance model

Condition	Irrigation category	Irrigation amount
$(\mathrm{pd\_def})_i \geq 0.75 \times (\mathrm{pd\_lim})_i$	High irrigation (HI)	$0.75 \times (\mathrm{pd\_lim})_i$
$0.5 \times (\mathrm{pd\_lim})_i \leq (\mathrm{pd\_def})_i < 0.75 \times (\mathrm{pd\_lim})_i$	Medium irrigation (MI)	$0.50 \times (\mathrm{pd\_lim})_i$
$0.25 \times (\mathrm{pd\_lim})_i \leq (\mathrm{pd\_def})_i < 0.5 \times (\mathrm{pd\_lim})_i$	Low irrigation (LI)	$0.25 \times (\mathrm{pd\_lim})_i$
$(\mathrm{pd\_def})_i < 0.25 \times (\mathrm{pd\_lim})_i$	No irrigation (NI)	0.00

Note: $(\mathrm{pd\_def})_i$ = deficit ponding depth estimated from water balance model for a given growth stage, i; and $(\mathrm{pd\_lim})_i$ = limiting ponding depth for a given growth stage, i (Refer to Table 1).

Crop yield at the end of each growth stage is computed using a simple growth algorithm and given by

$$\left(1 - \frac{Y_a^k}{Y_p^k}\right) = K_y^k \left(1 - \frac{\sum ET_a^k}{\sum ET_p^k}\right) \quad (11)$$

where Y_a^k and Y_p^k correspond to actual and potential above-ground biomass for a given growth stage 'k', respectively, K_y^k is the yield response factor for growth stage 'k' (Table 1), $\sum ET_a^k$ and $\sum ET_p^k$ correspond to actual and potential cumulative ET, respectively, from the beginning of crop season to the current growth stage 'k'. A number of researchers have demonstrated the efficacy of simple transpiration or ET-based crop growth models in simulating biomass and crop yield (Pereira et al. 2003; Choudhury and Singh 2016; Cao et al. 2019; Foster et al. 2017). All simulations were performed using Microsoft Excel, with source code and results available at: Github link https://github.com/ShubhamGedam/AgriIITH.

Results and Discussion

Analysis of IMD Forecasts

One-to-one association of rainfall forecasts with observed values and its temporal distribution are analyzed via scatter and time-series plots, respectively (Fig. 2). Both plots suggest a significant number of 'zero' rainy days happening during the non-monsoon period. High precipitation values were observed during the monsoon period. This is true for this part of the region; thus, the results indicate the forecast's ability to capture both daily and seasonal variations. However, the number of forecasted zero rainy days are relatively low (248 to 270 for different forecast lead times) as compared to the observed zero rainy days, i.e., 310. Only a few

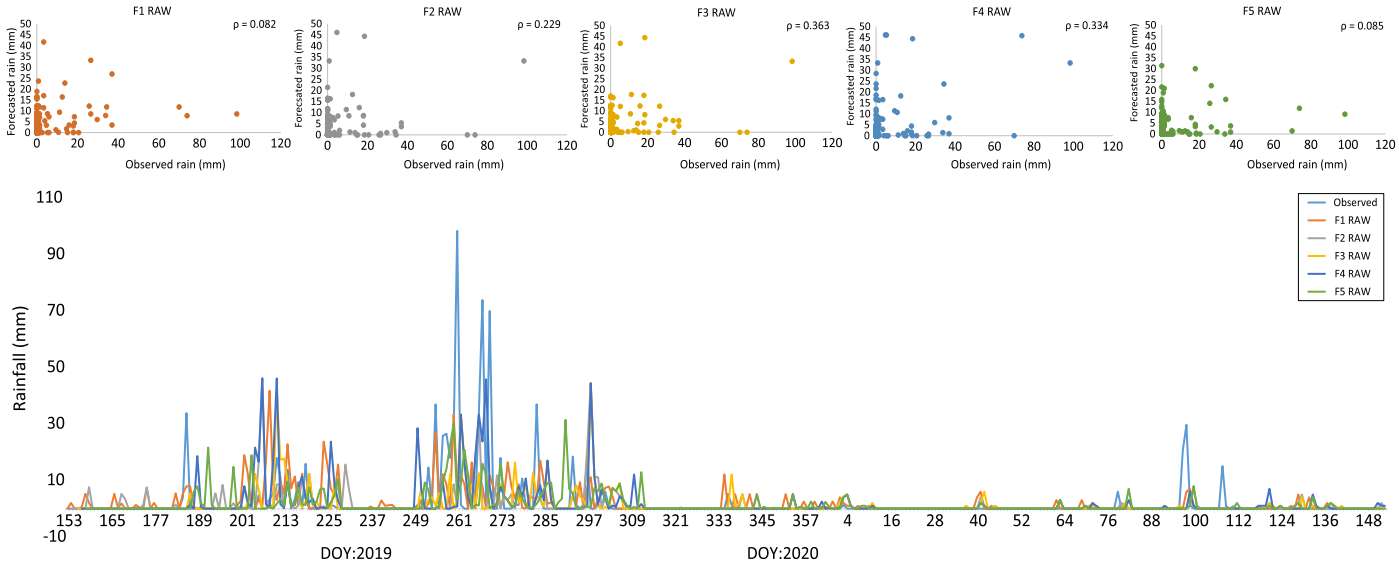

Fig. 2. Temporal distribution of observed and IMD-published forecasts of precipitation at different lead times. Inset: Scatterplots showing the correspondence between two datasets.

forecasts were correctly mapped with observed zero rainy days. This is seen in terms of non-zero (zero) rainfall forecasts corresponding to zero (non-zero) observed rainfall in scatterplots. This concludes that the number of misses and false alarms with zero precipitation are relatively high. The one-to-one correspondence between forecast and observed rainfall values is quantified using the Pearson correlation coefficient (ρ), and is found to be 0.35, 0.28, 0.36, 0.41, and 0.26 for 1 to 5 days lead time, respectively. Cumulative precipitation observed during Kharif (monsoon) and Rabi (winter) seasons are 643 mm and 8 mm, respectively, which are 6.25% and 91.1% less than the normal rainfall for the respective seasons. The site has recorded their highest daily rainfalls in 100 years in September, and the IMD forecasts did not capture it (top rows in Fig. 2). Removing these three highest daily rainfall values has significantly increased the ρ values to 0.98, 0.95, 0.97, 0.96, and 0.94, when only calculated for rainy days. Both rainfall magnitude and number of rainy days were underestimated at all lead times with a bias ranging from 0.39 to 0.76.

The reference ET (ET_0) is typically estimated using solar radiation (R_n); however, we used cloud cover (CC) data in lieu of R_n for effective utilization of IMD forecast data. ET_0 computed from CC forecasts agrees with those computed from observed R_n datasets ($\rho = 0.8$, RMSE $= 8.32$ mm). A good agreement between observed and forecasted ET_0 was observed due to non-zero, close range (1.5 to 6 mm) datasets. This concludes that the analytical method proposed by Cai et al. (2007) can be used to estimate ET_0 forecasts. Similar to rainfall, scatter plots and time-series plots were developed to compare forecast- and observed-ET_0 estimates (Fig. 3). As compared to 'P' forecasts, 'ET_0' forecasts appear to be more reliable, i.e., the values were scattered around the 1:1 line. This is reflected in medium- to high-correlation coefficient values, i.e., ρ values of 0.60, 0.58, 0.60, 0.60, and 0.58 observed for 1 to 5 days lead time, respectively. The time-series plots suggest high ET_0 in summer months followed by low ET_0 in winter months, which is consistent with literature (Goparaju and Ahmad 2019; Tyagi et al. 2000).

Performance of Bias Correction Methods

Both raw- and bias-corrected P and ET_0 forecasts were evaluated using three indices, i.e., multiplicative bias, RMSE, and ρ (Figs. 4 and 5). Biases greater than one were observed for raw rainfall forecasts, and the values increased for the first three forecast lead days. Values greater than one imply overestimated forecasts, and the forecasts are relatively low by 30% or more, except for one and four lead days. The contrasts with RMSE values, which were found to be the same at all lead times implying similar accuracy in raw forecasts for all forecast lead days. The correlation coefficient values varied with lead time, but their low values indicate no significant one-to-one association. The bias-corrected forecasts exhibited decreased multiplicative bias and no change in one-to-one association

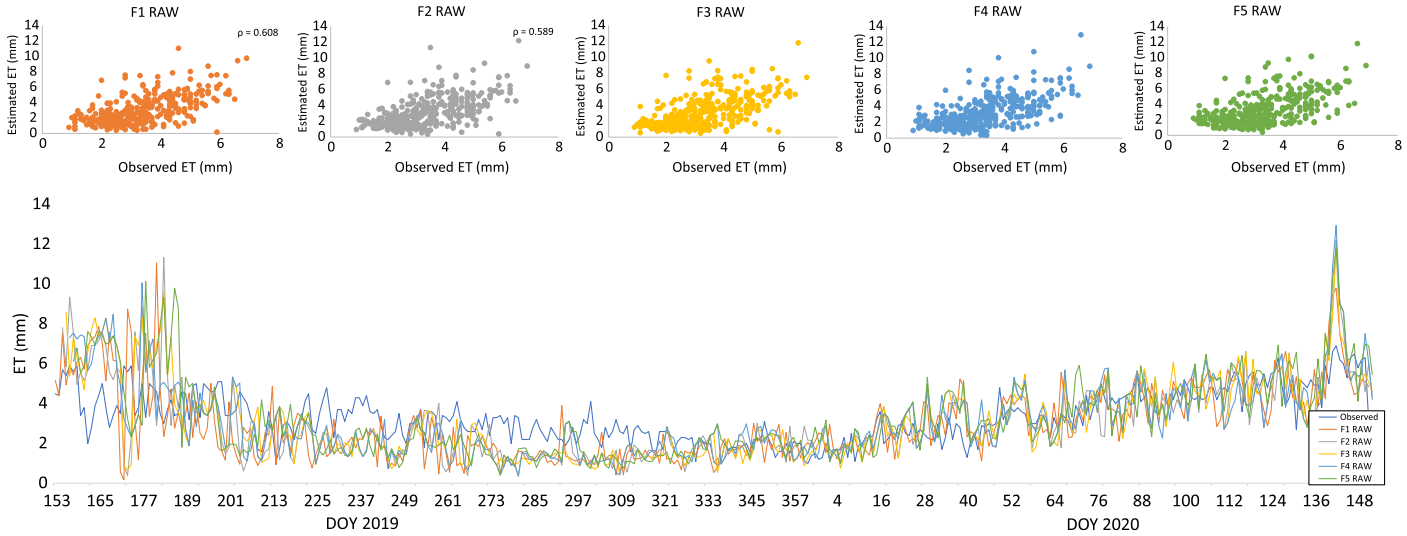

Fig. 3. Temporal distribution of observed and IMD-derived forecasts of evapotranspiration at different lead times. Inset: Scatterplots showing the correspondence between two datasets.

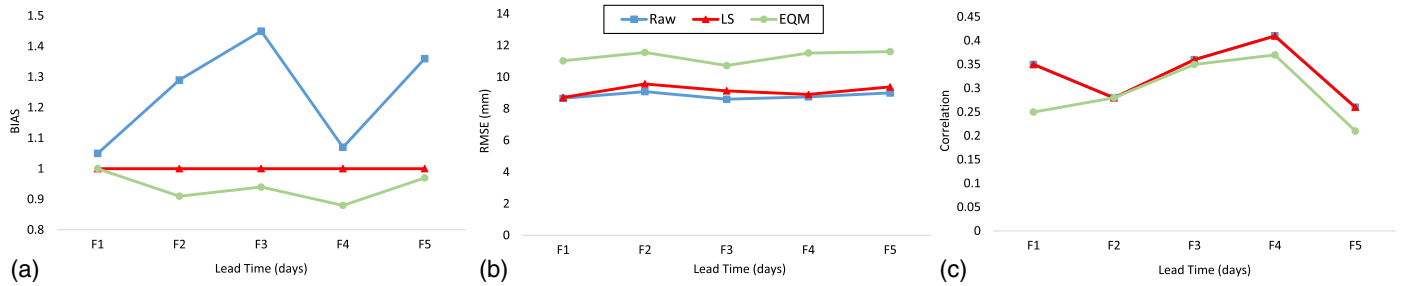

Fig. 4. Forecast skills of raw and bias-corrected precipitation as a function of lead time. Metrics considered include: (a) Bias; (b) RMSE; and (c) correlation coefficient (ρ).

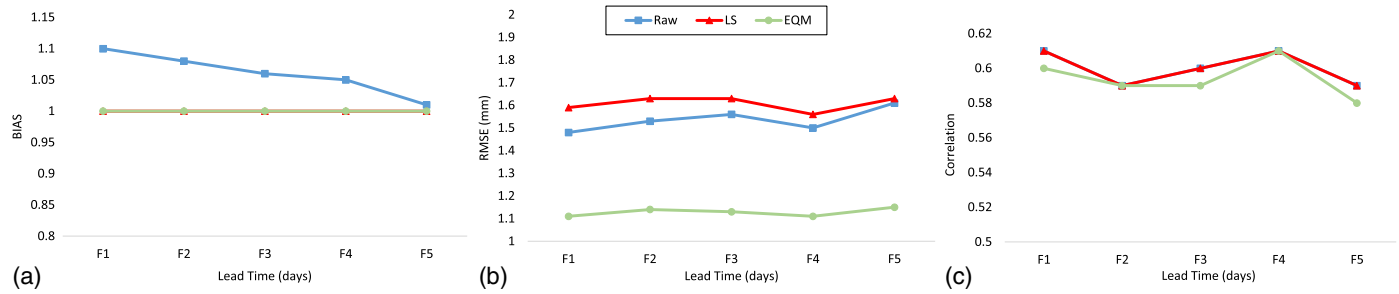

Fig. 5. Forecast skills of raw and bias-corrected evapotranspiration as a function of lead time. Metrics considered include: (a) Bias; (b) RMSE; and (c) correlation coefficient (ρ).

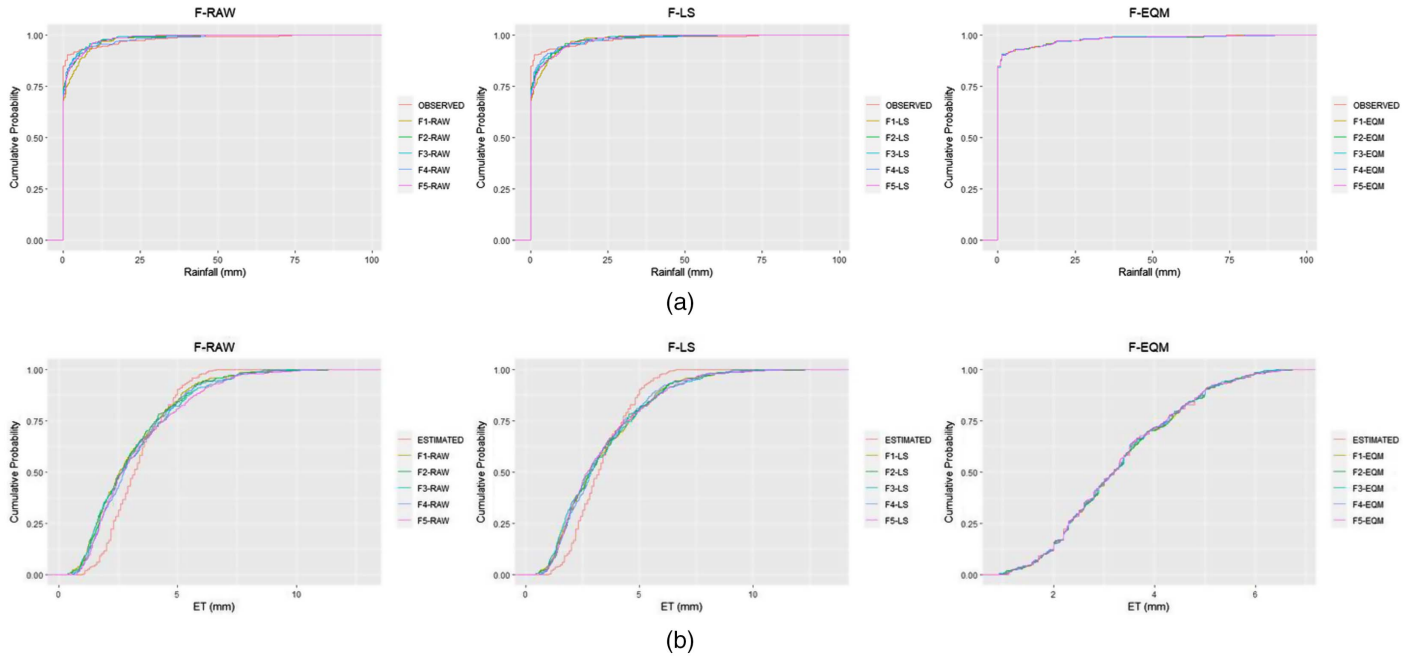

Fig. 6. Cumulative distribution functions (CDFs) of raw and bias-corrected forecasts of (a) precipitation; and (b) evapotranspiration with different lead times.

with the observed values. However, the EQM forecasts exhibited increased RMSE values. The results suggest no clear addition of value by bias correction techniques, and it may chiefly be due to the absence of bias (i.e., systematic pattern in error) and lack of information content in raw forecasts. Nonetheless, the bias correction techniques assisted in the increased performance of raw ET_0 forecasts. The raw ET_0 forecasts, unlike as one would expect, exhibited similar values for all three-verification metrics; note that the bias values are not significantly different, but interestingly decreased with increasing lead time. Both bias correction techniques removed the bias in raw forecasts at all lead times, whereas the EQM-corrected forecasts resulted in much lower RMSE values, unlike the LS-corrected forecasts, which resulted in slightly increased RMSE values. No significant changes in correlation values suggested no improvement in performance in one-to-one association. As crop yield is influenced by meteorological processes and irrigation schedule over a period of time, i.e., around 120 days, it is intuitive and important to analyze whether the forecasts map onto the observed values in their various distributional aspects. In this regard, cumulative density functions (CDFs) were developed for both observed values, raw forecasts and biased forecasts, of P and ET_0 for each lead time (Fig. 6). The CDF of observed rainfall suggests zero rainfall for much of the year, i.e., 80% of the time, whereas the CDF of raw forecasts suggests zero rainfall for relatively decreased percentage of time. Close observations of the CDFs reveal the following: (1) raw forecasts of lead time of one day are different from the forecasts of other lead times for non-zero rainfall amounts; (2) smaller rainfall amounts are less likely as compared to the higher rainfall amounts for raw forecasts; (3) approximately similar CDFs for both LS-corrected and raw forecasts; (4) approximately similar CDFs for both observed and EQM-corrected forecasts at all lead times. The above observations suggest an inability of raw forecasts and LS-corrected forecasts to match the distributional properties of observed rainfall, while the EQM-corrected forecast is able to match this property. As compared to rainfall CDFs, ET_0CDFs are widely spread and reflect a wide range of ET_0 values. The CDFs of raw forecasts at all lead times are approximately similar but significantly different from the CDFs of observed values. Similar to rainfall forecasts, LS techniques did not modify the CDFs of raw forecasts for ET_0; however, the EQM-adjusted forecast closely matches the corresponding observed values. These results suggest preserving the distributional

properties of the observed values in EQM-adjusted forecasts for both rainfall and ET_0, which results in increased accuracy for ET_0 forecasts.

Model Calibration

The performance of the crop coefficient-assisted FAO Penman–Monteith method to estimate actual ET (ET_a) was evaluated in comparison with eddy covariance (EC) flux observations. Prior to calibration, the quality of EC measurements was assessed by linearly regressing the available energy (R_n-G) with the turbulent fluxes ($H + LE$) considering daytime unstable flux measurements. The slope and intercept of the best fit line were found to be 0.76, 28.80 for Kharif season, and 0.86, 10.62 for Rabi season, respectively. Model calibration ensured changing the stage-specific crop coefficients (Table 1) and the AM parameters used in converting the cloud cover data into solar radiation. Fig. 7 compares the daily means of ET_a estimated from the FAO-K_c approach with flux tower observations for two crop seasons. Cumulative ET_a during Kharif season (383 mm) was found to be higher than in Rabi season (269 mm) due to favorable agro-climatic conditions (high VPD). We observed a close agreement between estimated and observed ET_a fluxes during both Kharif ($R^2 = 0.63$, NSE = 0.53, RMSE = 0.47 mm) and Rabi ($R^2 = 0.82$, NSE = 0.75, RMSE = 0.52 mm) seasons.

Comparison of Irrigation Scenarios

Conventional irrigation (CI) and hypothetical forecast (HF) scenarios only use observed weather data for water balance and crop growth simulations. The two scenarios can also be considered as a benchmark to define the two extreme irrigation treatments (CI for highest water use with low yield, and HF for lowest water use with high yield). Fig. 8 represents the stage-wise accumulation of major water fluxes (irrigation and deep percolation) and relative yield for the two extreme treatments. CI has resulted in the highest use of irrigation water at all growth stages, accumulating to 820 mm in Kharif and 880 mm in Rabi seasons. The corresponding values with the HF scenario are 660 mm and 710 mm, respectively. A high irrigation amount in Rabi season can be attributed to low rainfall. Deep percolation with CI accounts for 1,140 mm in Kharif and 680 mm in Rabi season. The corresponding values with HF are 980 mm and 500 mm, respectively. Due to a high, uneven rainfall distribution, a high percolation in excess of irrigation was observed in the Kharif season. We observed a steep rise in deep percolation during vegetative and reproduction stages for both seasons. Due to the low crop water requirements, both irrigation (62.50 ± 27.5 mm) and deep percolation (196.26 ± 175.8 mm) are minimal during the ripening stage. Deep percolation as a fraction of total water applied (P+I) was found to be 76.5% with CI and 69.5% with HF. This concludes that a significant amount of DP can be saved by the effective utilization of weather parameters. For ease of comparison,

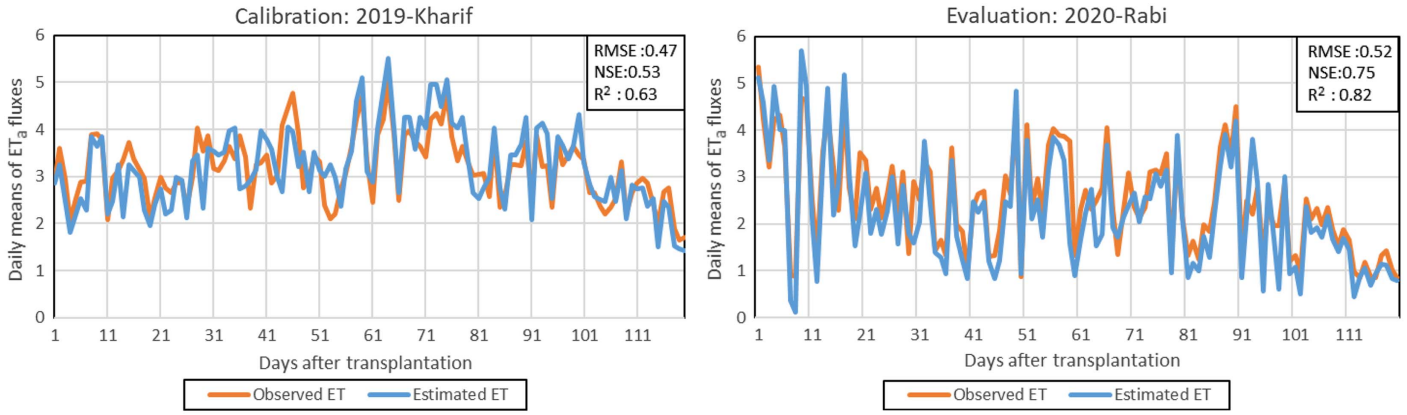

Fig. 7. Calibration (period: 2019-Kharif) and evaluation (period: 2020-Rabi) of water balance model for daily means of ET_a fluxes against the flux tower observations. Model performance is evaluated using the residual statistical indices including R^2, NSE, and RMSE.

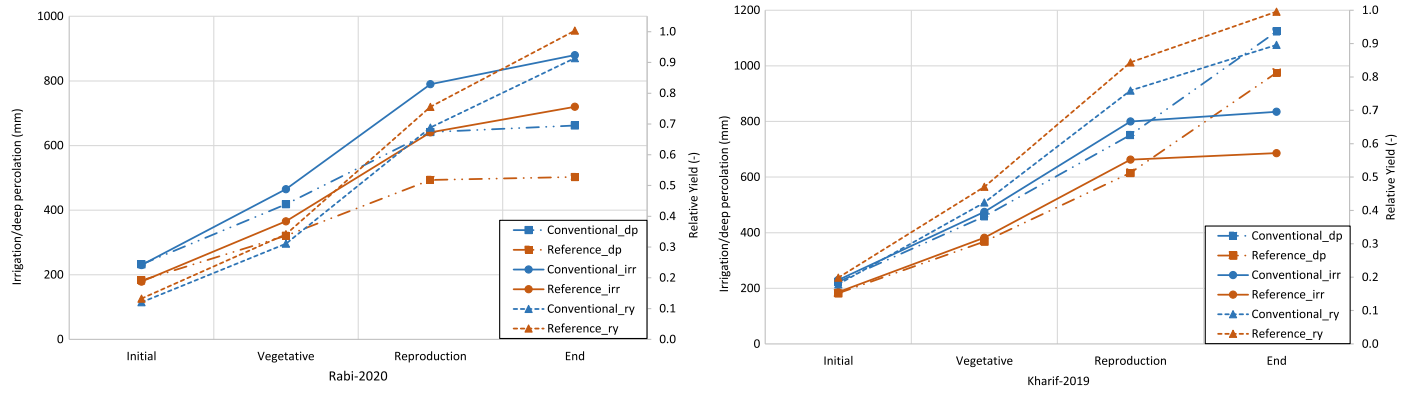

Fig. 8. Stage-wise accumulation of irrigation water (irr), deep percolation (dp), and relative yield (ry) for conventional and reference (hypothetical, 5-day perfect forecast) irrigation scenarios as represented in two different hues, for the two growing seasons: (a) Rabi; and (b) Kharif.

we assumed the highest yield was achieved with the HF scenario, resulting in a relative yield (RY) of 1.0. Accordingly, CI has resulted in a RY of 0.88 in Kharif and 0.87 in Rabi, slightly lower than the potential yield observed in the region (3,040 kg ha^{-1} in Kharif and 2,462 kg ha^{-1} in Rabi). CI with rule-based irrigation decisions based on farmers experience has consumed 733 mm and 895 mm of irrigation water during Kharif and Rabi seasons, respectively. Deep percolation by this method amounts to 1,035 mm and 679 mm during Kharif and Rabi seasons, respectively. This concludes that farmers' experience in considering rule-based irrigation can slightly minimize irrigation amounts and deep percolation losses, particularly during Kharif season.

By considering raw and bias-corrected forecasts with different lead times, components of water balance for the Kharif season are presented in Fig. 9. Except at 1-day lead times, the raw forecasts have underestimated the precipitation, thereby utilizing higher irrigation amounts. Precipitation and ET_a contributed to 39.7% ± 6.51% and 25.1% ± 1.82% of the total water balance, respectively. While precipitation showed a general decreasing trend with lead time, we could not observe a clear pattern. ET_a has shown a clear increasing trend with lead time. Overall, deep percolation using the forecasted datasets was found to be significantly lower than the CI scenario and marginally lower than the HF scenario. This concludes that raw forecasts can minimize the deep percolation losses at the cost of increasing the irrigation. It can also be observed that relative yield was not compromised with raw forecast information. The LS-corrected precipitation values are much closer to the HF scenario than raw forecasts, thus lowering the irrigation amounts. Deep percolation with LS corrections are in the range of 910 to 1,010 mm, with the HF-derived value falling in between. This concludes that LS-corrected forecasts result in water balance fluxes that are close to the reference values. We observed a surge in the EQM-corrected precipitation values (910 to 1,320 mm) at all lead times; these values are impractical, hence resulting in spurious deep percolation values that are 31% to 53% higher than the reference value, respectively. EQM correction has decreased the performance of irrigation schedules due to a large number of mismatched pairs of 'zero' precipitations both in the observed and raw forecasts. IMD weather forecasts with LS bias correction have outperformed all other scenarios with a 15%–28% savings in irrigation water and 10%–19% savings in deep percolation over CI.

In considering raw and bias-corrected forecasts with different lead times, the components of water balance for the Rabi season are presented in Fig. 10. Precipitation and ET_a contributed to 4.8% ± 1.32% and 31.6% ± 0.96% of the total water balance, respectively. Even though the raw forecasts have overestimated the precipitation at all lead times, their magnitude is significantly low (50 ± 6 mm). Since the contribution of precipitation to the total water balance is very low, both irrigation and deep percolation were fairly constant at all lead times and are in close agreement with the two extreme scenarios (CI and HF). LS-corrected forecasts have slightly increased the precipitation but could not alter the other fluxes. We observed a similar response with EQM-corrected irrigation scenarios. Overall, the water balance components of all forecast scenarios are closer to the CI values, concluding that the irrigation schedules are insensitive to weather forecasts (with or without bias correction) for the Rabi season. A low magnitude of highly uncertain variable precipitation along with a highly consistent and stable ET_a data has made Rabi season less dependent on weather forecasts for irrigation scheduling.

Though LS- and EQM-corrected forecasts have slightly improved the forecasting skill (Figs. 4 and 5), their performance with

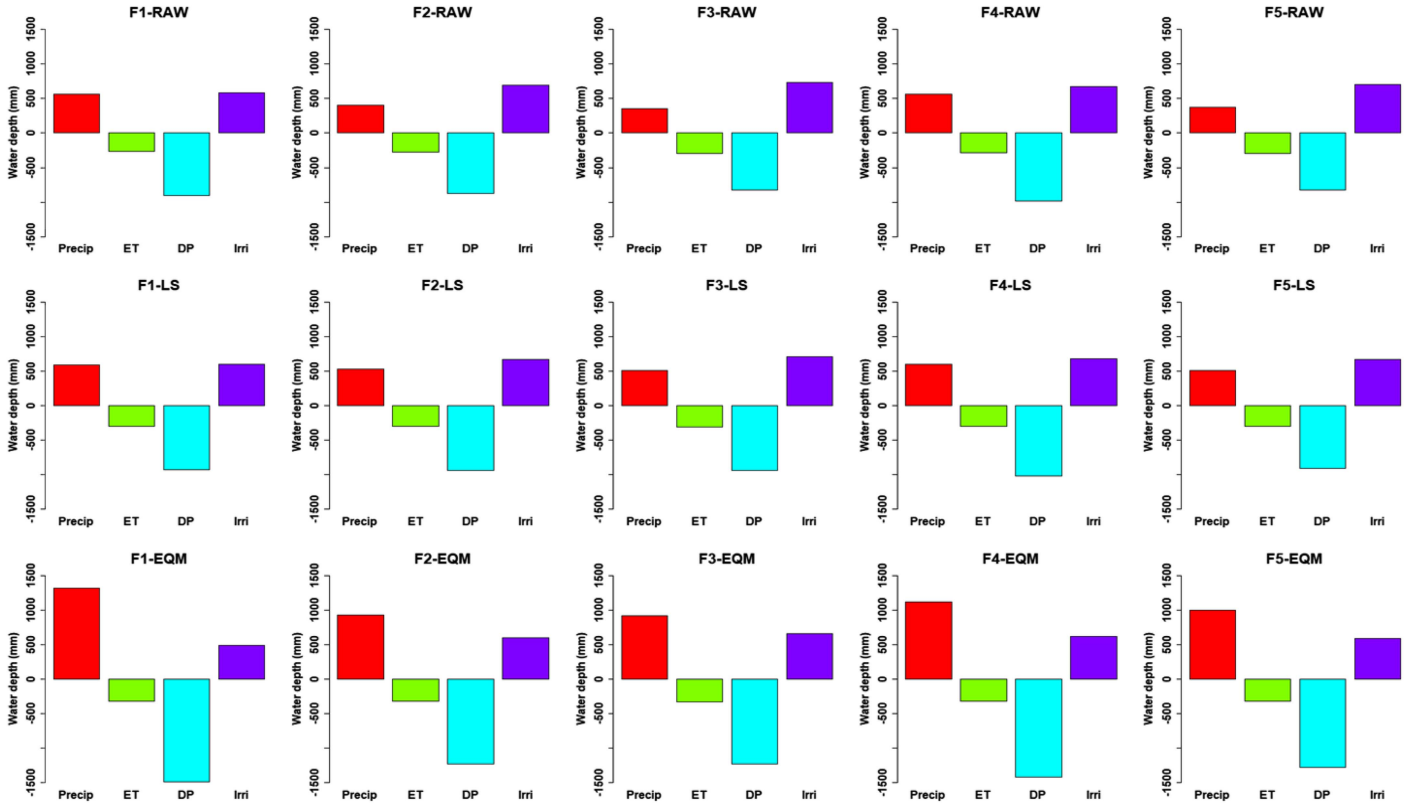

Fig. 9. Components of water balance for the 2019-Kharif season rice crop considering: IMD raw forecasts (F-RAW), LS bias-corrected forecasts (F-LS), and EQM bias-corrected forecasts (F-EQM) with different lead times.

J. Water Resour. Plann. Manage., 2023, 149(2): 04022079

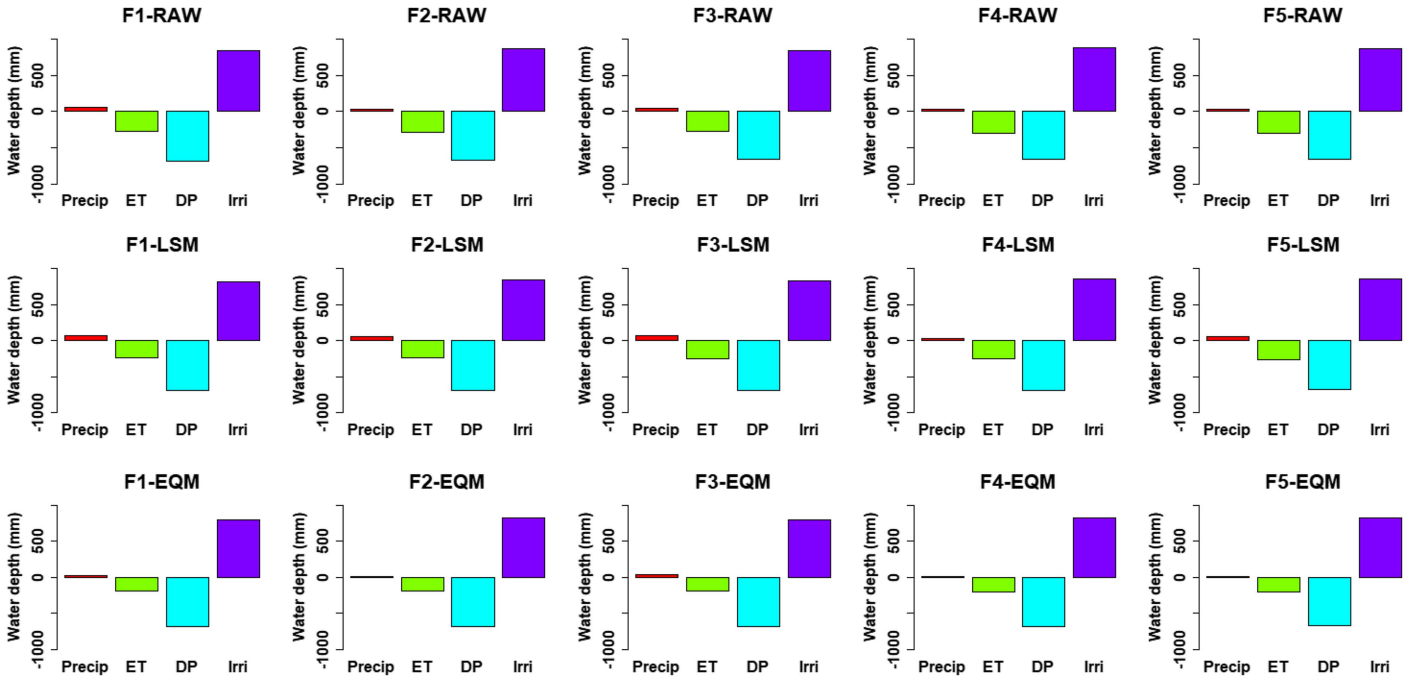

Fig. 10. Components of water balance for the 2020-Rabi season rice crop considering: IMD raw forecasts (F-RAW), LS bias-corrected forecasts (F-LS), and EQM bias-corrected forecasts (F-EQM) with different lead times.

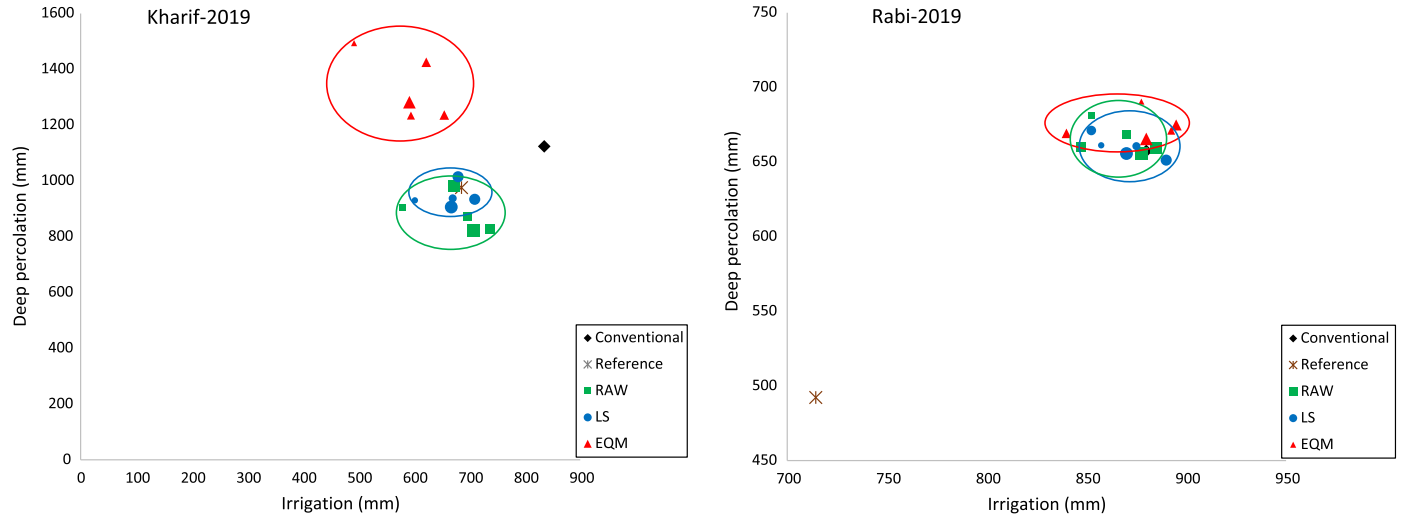

Fig. 11. Cluster representation of major water balance fluxes (irrigation and deep percolation) considering raw forecasts (green), LS-corrected forecasts (blue), and EQM-corrected forecasts (red) with different lead times. For each forecast scenario, graduate symbols were used to relate the size to the forecast horizon.

irrigation and crop growth models is antithetical (Fig. 11). While LS correction has improved the performance of the irrigation model, EQM correction has resulted in spurious percolation losses inferior to raw forecast scenarios. This concludes that selecting the appropriate bias correction technique is vital for the improvement of irrigation schedules. Due to averaging over the forecast horizon, a close cluster of data points for each scenario (Fig. 11) concludes that the inaccuracies in weather forecast will diminish as they propagate into irrigation models.

Selection of Optimal Forecast Scenario

Conventional and forecast-driven irrigation scenarios were evaluated in relation to HF, which is considered a benchmark (Fig. 11). All scenarios were evaluated by comparing the deviation in major water fluxes (irrigation and deep percolation) from HF outputs. Irrigation and DP for the HF scenario (marked as '*') during Kharif season are 680 mm and 980 mm, respectively. The corresponding values for the CI scenario (marked as '◆') are 820 mm and 1140 mm. This concludes that CI has resulted in a 20% waste of irrigation water and 16% waste of DP due to ignoring perfect weather forecast information and rule-based decisions. Except for EQM-corrected forecasts, all other scenarios have performed better than CI, of which, the LS-corrected forecasts have resulted in a close match of water fluxes with the HF scenario. It should be noted that savings in irrigation water and deep percolation are attributed to the effect of considering weather forecasts in conjunction with

rule-based irrigation. Our results conclude that IMD forecasts at multiple lead times can significantly improve irrigation scheduling by saving 28% ± 6% irrigation water and 17% ± 5% DP and improving the relative yield by 2%. Water savings can be improved further with LS-corrected irrigation scenarios. Also, variability in the estimated water fluxes between the lead times is minimized with the LS-corrected scenario. Irrigation and DP for the HF scenario during Rabi season are 710 mm and 500 mm, respectively. Both raw and bias-corrected forecasts have significantly deviated from HF results, with high irrigation (860 ± 25 mm) and DP (660 ± 35 mm) fluxes. A high offset from the HF scenario can be attributed to low cumulative precipitation, both in the observed (8 mm) and IMD-forecasted (45 ± 12 mm) datasets. This has significantly overestimated the irrigation and DP values at all lead times. Our results conclude that IMD forecasts with or without bias correction provide no additional value to irrigation scheduling in the Rabi season. The contribution of 'P' to the water balance fluxes plays a significant role in deciding the role of weather forecasts on improved irrigation schedules and crop yield.

Due to resource constraints, we considered the data of only two irrigation seasons. Considering long-term data across multiple years (dry, normal, wet) may improve our findings, which can be taken up in future. Since irrigation via free power has no associated cost in Indian setting, we have not analyzed the cost benefits of using weather forecasts. We have considered deterministic, numerical forecasts as published by IMD. A binomial or categorical representation of IMD forecasts (ex: rain versus no-rain condition) may help in scheduling irrigation and easing field implementation.

Conclusions

This research is aimed at assessing the performance of IMD short-term forecasts of 'P' and 'ET_o' when used in irrigation schedules and crop growth models. Forecasting skills for both variables was found to be low at all lead times. We observed a marginal improvement in the forecasting skill of P with LS bias correction, whereas EQM correction did not show much improvement. A high RMSE (8 mm at a 2-day lead time to 25 mm at a5-day lead time) was observed with raw P forecasts due to a systematic underestimation, which was marginally improved after bias correction. The Mann–Whitney rank sum test on bias-corrected and raw forecasts of 'P' and ET_o concluded that bias-corrected 'P' at all lead times, LS-corrected ET_o at a 1-day lead time, and EQM-corrected ET_o at all lead times are significantly different from their respective observations at 95% significance level. CDFs for raw and forecasts of P and ET_o revealed that bias correction is hardly improved the performance of the P forecast and significantly improved the performance of the ET_o forecast. The model was calibrated and evaluated with observed ET with a flux tower and showed a good correspondence (NSE = 0.625, $R^2 = 0.72$, RMSE = 0.49 mm). IMD weather forecasts for Kharif season with LS bias correction outperformed other scenarios with approximately 15% to 28% savings in irrigation water and 10 to 19% savings in deep percolation over CI. This scenario was reversed for Rabi season, where the irrigation schedules were found to be insensitive to weather forecasts (with or without bias correction). All scenarios were compared with HF outputs of irrigation and deep percolation. Our results conclude that CI has resulted in 20% waste of irrigation water and 16% waste of DP due to ignoring weather forecast information. IMD forecasts at multiple lead times can significantly improve the irrigation scheduling by saving 28% ± 6% irrigation water and 17% ± 5% DP and improving the relative yield by 2%.

Data Availability Statement

Some or all the data along with the model code used in this study can be obtained from the corresponding author upon reasonable request. Following datasets/simulation files are available in the online repository (https://github.com/ShubhamGedam/AgriIITH).

1. Daily observations of meteorological datasets.
2. IMD-published rainfall with 1 to 5 day lead times (raw, bias-corrected).
3. Penman–Monteith Estimates of ET for 1 to 5 day lead times (raw, bias-corrected).
4. Daily water balance fluxes for each irrigation scenario (CI, F-RAW, F-LS, F-EQM, HF).

Acknowledgments

The authors acknowledge the services of Dr. Sarah Kamala Kumari Mylabathula, Department of English and Humanities, MVGR College of Engineering, Vizianagaram for proofreading the manuscript. The authors also acknowledge the anonymous reviewers for their insightful comments. This research evolved as an extension of a term project in CE6520-Irrigation Water Management course at IIT Hyderabad.

References

Aggarwal, P. K. 2008. "Global climate change and Indian agriculture: Impacts, adaptation and mitigation." *Indian J. Agric. Sci.* 78 (11): 911.

Allen, R. G., et al. 2006. "A recommendation on standardized surface resistance for hourly calculation of reference ETo by the FAO56 Penman-Monteith method." *Agric. Water Manage.* 81 (1–2): 1–22. https://doi.org/10.1016/j.agwat.2005.03.007.

Allen, R. G., L. S. Pereira, D. Raes, and M. Smith. 1998. *Crop evapotranspiration—Guidelines for computing crop water requirements—FAO Irrigation and drainage paper 56*, D05109. Rome: Food and Agriculture Organization.

Anupoju, V., B. P. Kambhammettu, and S. K. Regonda. 2021. "Role of short-term weather forecast horizon in irrigation scheduling and crop water productivity of rice." *J. Water Resour. Plann. Manage.* 147 (8): 05021009. https://doi.org/10.1061/(ASCE)WR.1943-5452.0001406.

Anupoju, V., and B. V. N. P. Kambhammettu. 2020. "Role of deficit irrigation strategies on ET partition and crop water productivity of rice in semi-arid tropics of south India." *Irrig. Sci.* 38 (4): 415–430. https://doi.org/10.1007/s00271-020-00684-1.

Arnell, N. W. 2003. "Relative effects of multi-decadal climatic variability and changes in the mean and variability of climate due to global warming: Future streamflows in Britain." *J. Hydrol.* 270 (3–4): 195–213. https://doi.org/10.1016/S0022-1694(02)00288-3.

Auffhammer, M., V. Ramanathan, and J. R. Vincent. 2006. "Integrated model shows that atmospheric brown clouds and greenhouse gases have reduced rice harvests in India." *Proc. Natl. Acad. Sci. U.S.A.* 103 (52): 19668–19672. https://doi.org/10.1073/pnas.0609584104.

Ballesteros, R., J. F. Ortega, and M. Á. Moreno. 2016. "FORETo: New software for reference evapotranspiration forecasting." *J. Arid. Environ.* 124 (Jan): 128–141. https://doi.org/10.1016/j.jaridenv.2015.08.006.

Boutraa, T. 2010. "Improvement of water use efficiency in irrigated agriculture: A review." *J. Agron.* 9 (1): 1–8. https://doi.org/10.3923/ja.2010.1.8.

Cai, J., Y. Liu, T. Lei, and L. S. Pereira. 2007. "Estimating reference evapotranspiration with the FAO Penman–Monteith equation using daily weather forecast messages." *Agric. For. Meteorol.* 145 (1–2): 22–35. https://doi.org/10.1016/j.agrformet.2007.04.012.

Cai, X., M. I. Hejazi, and D. Wang. 2011. "Value of probabilistic weather forecasts: Assessment by real-time optimization of irrigation scheduling." *J. Water Resour. Plann. Manage.* 137 (5): 391–403. https://doi.org/10.1061/(ASCE)WR.1943-5452.0000126.

Cao, J., J. Tan, Y. Cui, and Y. Luo. 2019. "Irrigation scheduling of paddy rice using short-term weather forecast data." *Agric. Water Manage.* 213 (Mar): 714–723. https://doi.org/10.1016/j.agwat.2018.10.046.

CGWB (Central Ground Water Board). 2013. *Ground water brochure*. Medak, Andhra Pradesh, India: CGWB.

Chapagain, A. K., and A. Y. Hoekstra. 2011. "The blue, green and grey water footprint of rice from production and consumption perspectives." *Ecol. Econ.* 70 (4): 749–758. https://doi.org/10.1016/j.ecolecon.2010.11.012.

Chen, H., L. Sun, R. Cifelli, and P. Xie. 2021. "Deep learning for bias correction of satellite retrievals of orographic precipitation." *IEEE Trans. Geosci. Remote Sens.* 60: 1–11. https://doi.org/10.1109/TGRS.2021.3105438.

Chen, J., F. P. Brissette, D. Chaumont, and M. Braun. 2013a. "Finding appropriate bias correction methods in downscaling precipitation for hydrologic impact studies over North America." *Water Resour. Res.* 49 (7): 4187–4205. https://doi.org/10.1002/wrcr.20331.

Chen, J., F. P. Brissette, D. Chaumont, and M. Braun. 2013b. "Performance and uncertainty evaluation of empirical downscaling methods in quantifying the climate change impacts on hydrology over two North American river basins." *J. Hydrol.* 479 (Feb): 200–214. https://doi.org/10.1016/j.jhydrol.2012.11.062.

Choudhury, B. U., and A. K. Singh. 2016. "Estimation of crop coefficient of irrigated transplanted puddled rice by field scale water balance in the semi-arid Indo-Gangetic Plains, India." *Agric. Water Manage.* 176 (Oct): 142–150. https://doi.org/10.1016/j.agwat.2016.05.027.

Cline, W. R. 2007. *Global warming and agriculture: Impact estimates by country.* Washington, DC: Peterson Institute.

Crochemore, L., M. H. Ramos, and F. Pappenberger. 2016. "Bias correcting precipitation forecasts to improve the skill of seasonal streamflow forecasts." *Hydrol. Earth Syst. Sci.* 20 (9): 3601–3618. https://doi.org/10.5194/hess-20-3601-2016.

Dang, Q. T., P. Laux, and H. Kunstmann. 2017. "Future high and low flow estimations for central Vietnam: A hydrometeorological modelling chain approach." *Hydrol. Sci. J.* 62 (11): 1867–1889. https://doi.org/10.1080/02626667.2017.1353696.

FAO (Food and Agricultural Organization). 2017. *AQUASTAT database, Agriculture water withdrawal*. Rome: FAO.

Foster, T., N. Brozović, A. P. Butler, C. M. U. Neale, D. Raes, P. Steduto, E. Fereres, and T. C. Hsiao. 2017. "AquaCrop-OS: An open source version of FAO's crop water productivity model." *Agric. Water Manage.* 181 (Feb): 18–22. https://doi.org/10.1016/j.agwat.2016.11.015.

Goparaju, L., and F. Ahmad. 2019. "Analyzing the risk related to Climate Change attributes and their impact, a step towards Climate-Smart Village (CSV): A geospatial approach to bring geoponics sustainability in India." *Spatial Inf. Res.* 27 (6): 613–625. https://doi.org/10.1007/s41324-019-00258-0.

Hejazi, M. I., X. Cai, X. Yuan, X. Z. Liang, and P. Kumar. 2014. "Incorporating reanalysis-based short-term forecasts from a regional climate model in an irrigation scheduling optimization problem." *J. Water Resour. Plann. Manage.* 140 (5): 699–713. https://doi.org/10.1061/(ASCE)WR.1943-5452.0000365.

Ines, A. V., and J. W. Hansen. 2006. "Bias correction of daily GCM rainfall for crop simulation studies." *Agric. For. Meteorol.* 138 (1–4): 44–53. https://doi.org/10.1016/j.agrformet.2006.03.009.

Jamal, A., R. Linker, and M. Housh. 2018. "Comparison of various stochastic approaches for irrigation scheduling using seasonal climate forecasts." *J. Water Resour. Plann. Manage.* 144 (7): 04018028. https://doi.org/10.1061/(ASCE)WR.1943-5452.0000951.

Jamal, A., R. Linker, and M. Housh. 2019. "Optimal irrigation with perfect weekly forecasts versus imperfect seasonal forecasts." *J. Water Resour. Plann. Manage.* 145 (5): 06019003. https://doi.org/10.1061/(ASCE)WR.1943-5452.0001066.

Kottek, M., J. Grieser, C. Beck, B. Rudolf, and F. Rubel. 2006. "World map of the Köppen-Geiger climate classification updated." *Meteorologische Zeitschrift* 15: 259–263. https://doi.org/10.1127/0941-2948/2006/0130.

Kumar, M., N. S. Raghuwanshi, R. Singh, W. W. Wallender, and W. O. Pruitt. 2002. "Estimating evapotranspiration using artificial neural network." *ASCE J. Irrig. Drain. Eng.* 128 (4): 224–233. https://doi.org/10.1061/(ASCE)0733-9437(2002)128:4(224).

Lafon, T., S. Dadson, G. Buys, and C. Prudhomme. 2013. "Bias correction of daily precipitation simulated by a regional climate model: A comparison of methods." *Int. J. Climatol.* 33 (6): 1367–1381. https://doi.org/10.1002/joc.3518.

Landeras, G., A. Ortiz-Barredo, and J. J. López. 2009. "Forecasting weekly evapotranspiration with ARIMA and artificial neural network models." *J. Irrig. Drain. Eng.* 135 (3): 323–334. https://doi.org/10.1061/(ASCE)IR.1943-4774.0000008.

Luo, Y., X. Chang, S. Peng, S. Khan, W. Wang, Q. Zheng, and X. Cai. 2014. "Short-term forecasting of daily reference evapotranspiration using the Hargreaves–Samani model and temperature forecasts." *Agric. Water Manage.* 136 (Apr): 42–51. https://doi.org/10.1016/j.agwat.2014.01.006.

Maity, R., M. Suman, P. Laux, and H. Kunstmann. 2019. "Bias correction of zero-inflated RCM precipitation fields: A copula-based scheme for both mean and extreme conditions." *J. Hydrometeorol.* 20 (4): 595–611. https://doi.org/10.1175/JHM-D-18-0126.1.

Mishra, A., C. Siderius, K. Aberson, M. Van der Ploeg, and J. Froebrich. 2013. "Short-term rainfall forecasts as a soft adaptation to climate change in irrigation management in North-East India." *Agric. Water Manage.* 127 (Sep): 97–106. https://doi.org/10.1016/j.agwat.2013.06.001.

Mukhopadhyay, S., J. O. Ogutu, G. Bartzke, H. T. Dublin, and H. P. Piepho. 2019. "Modelling spatio-temporal variation in sparse rainfall data using a hierarchical Bayesian regression model." *J. Agric. Biol. Environ. Stat.* 24 (2): 369–393. https://doi.org/10.1007/s13253-019-00357-3.

Nikolaou, G., D. Neocleous, A. Christou, E. Kitta, and N. Katsoulas. 2020. "Implementing sustainable irrigation in water-scarce regions under the impact of climate change." *Agronomy* 10 (8): 1120. https://doi.org/10.3390/agronomy10081120.

Pereira, L. S., P. R. Teodoro, P. N. Rodrigues, and J. L. Teixeira. 2003. "Irrigation scheduling simulation: The model ISAREG." In *Tools for drought mitigation in Mediterranean regions*, 161–180. Dordrecht, Netherland: Springer.

Pierce, D. W., D. R. Cayan, E. P. Maurer, J. T. Abatzoglou, and K. C. Hegewisch. 2015. "Improved bias correction techniques for hydrological simulations of climate change." *J. Hydrometeorol.* 16 (6): 2421–2442. https://doi.org/10.1175/JHM-D-14-0236.1.

Sharma, B. R., A. Gulati, G. Mohan, S. Manchanda, I. Ray, and U. Amarasinghe. 2018. *Water productivity mapping of major Indian crops*. New Delhi, India: National Bank for Agriculture and Rural Development.

Snyder, R. L., C. Palmer, M. Orang, and M. Anderson. 2009. "National weather service reference evapotranspiration forecast." *Crop Water Use* 4: 1–6.

Tiwari, A. D., P. Mukhopadhyay, and V. Mishra. 2022. "Influence of bias correction of meteorological and streamflow forecast on hydrological prediction in India." *J. Hydrometeorol.* 23 (7): 1171–1192. https://doi.org/10.1175/JHM-D-20-0235.1.

Traore, S., Y. Luo, and G. Fipps. 2016. "Deployment of artificial neural network for short term forecasting of evapotranspiration using public weather forecast restricted messages." *Agric. Water Manage.* 163 (Jan): 363–379. https://doi.org/10.1016/j.agwat.2015.10.009.

Tyagi, N. K., D. K. Sharma, and S. K. Luthra. 2000. "Determination of evapotranspiration and crop coefficients of rice and sunflower with lysimeter." *Agric. Water Manage.* 45 (1): 41–54. https://doi.org/10.1016/S0378-3774(99)00071-2.

Venäläinen, A., T. Salo, and C. Fortelius. 2005. "The use of numerical weather forecast model predictions as a source of data for irrigation modeling." *Meteorol. Appl.* 12 (4): 307–318. https://doi.org/10.1017/S135048270500188X.

Wang, D., and X. Cai. 2009. "Irrigation scheduling—Role of weather forecasting and farmers' behavior." *J. Water Resour. Plann. Manage.* 135 (5): 364–372. https://doi.org/10.1061/(ASCE)0733-9496(2009)135:5(364).

Xiong, Y., Y. Luo, Y. Wang, S. Traore, J. Xu, X. Jiao, and G. Fipps. 2016. "Forecasting daily reference evapotranspiration using the Blaney–Criddle model and temperature forecasts." *Arch. Agron. Soil Sci.* 62 (6): 790–805. https://doi.org/10.1080/03650340.2015.1083983.

Yang, Y., Y. Cui, K. Bai, T. Luo, J. Dai, W. Wang, and Y. Luo. 2019. "Short-term forecasting of daily reference evapotranspiration using the reduced-set Penman-Monteith model and public weather forecasts." *Agric. Water Manage.* 211 (Jan): 70–80. https://doi.org/10.1016/j.agwat.2018.09.036.

Yang, Y., Y. Cui, Y. Luo, X. Lyu, S. Traore, S. Khan, and W. Wang. 2016. "Short-term forecasting of daily reference evapotranspiration using the Penman-Monteith model and public weather forecasts." *Agric. Water Manage.* 177 (Nov): 329–339. https://doi.org/10.1016/j.agwat.2016.08.020.